Position Measurements with Micro-Channel Plates and Transmission lines using Pico-second Timing and Waveform Analysis

Bernhard Adams[a], Klaus Attenkofer[a], Mircea Bogdan[b], Karen Byrum[a], Jean-Francois C. Genat[b], Herve Grabas[c], Henry J. Frisch[b], Heejong Kim[b], Mary K. Heintz[b], Tyler Natoli[b], Richard Northrop[b], Eric Oberla[b], Samuel Meehan[b], Edward N. May[a], Robert Stanek[a], Fukun Tang[b], Gary Varner[d] and Eugene Yurtsev[a]

[a]Argonne National Laboratory, 9700, S. Cass Avenue, Argonne, IL 60439, USA
[b]University of Chicago, Enrico Fermi Institute, 5640 S. Ellis Av, Chicago IL 60637, USA
[c]Ecole Superieure d'Electricite, Gif-sur-Yvette, 91190, France
[d]University of Hawai'i, 2500 Campus Road, Honolulu, HI 96822, USA

genat@hep.uchicago.edu

Abstract

The anodes of Micro-Channel Plate devices are coupled to fast transmission lines in order to reduce the number of electronics readout channels, and can provide two-dimension position measurements using two-ends delay timing. Tests with a laser and digital waveform analysis show that resolutions of a few hundreds of microns along the transmission line can be reached taking advantage of a few pico-second timing estimation. This technique is planned to be used in Micro-channel Plate devices integrating the transmission lines as anodes.

I. INTRODUCTION

DELAY-LINE readout with pico-second timing resolution allows measuring the impact of a particle along a detector with a precision better than one millimetre. The time distance relation is:

$$\Delta t = 2\,\Delta x / v$$

where v is the propagation velocity of the pulse along the line.

As some photo-detector applications would cover tens of square meters, it is also important to reduce the number of electronics channels. Delay lines coupled to the detector and read at their two ends can reduce significantly this number, compared to full pixels detectors such as regular Micro Channel Plates available from the industry. The transmission lines could also be integrated with the photo-detector itself in order to reduce the physical dimensions and power, increase the analog bandwidth, improve the readout speed, and provide all-digital data output, when equipped with custom designed readout Application Specific Integrated Circuits (ASIC).

We present in this work position measurement results obtained with Micro-Channel Plate detectors tied to 50 Ω transmission lines implemented on high-frequency printed circuit boards, read with a fast digital oscilloscope.

II. EXPERIMENTAL SET-UP

Micro-Channel Plate tubes from Photonis X85011 and X85022 (resp. 25 and 10 μm pore size) of 2-inch x 2-inch size have been used in this work. A 25 μm MCP with 1024 anode pads is shown Figure 1. These MCPs have been connected to 50 Ohms transmission lines printed circuit cards and tested using a 408 nm wavelength laser focused on the window entrance of the MCP. The number of amplified photo-electrons is evaluated using a single photo electron sensitive photo-multiplier. Once the velocity along the 10 cm-long transmission line is determined, the position along the line is derived from the difference in delays between the two ends of the card. Since the signals at the two ends originate from the same pulse at the output of the MCP, their shapes are strongly correlated. Then, a waveform analysis using least square fits to a known template signal derived from the averaged measurements allows extracting the time of arrival of the pulse at the two ends of the line.

A transmission line printed circuit card has been designed using an RF ceramic substrate allowing reaching bandwidths up to 3 GHz. The tubes with 32 x 32 anodes have been glued to the transmission line card with conducting silver epoxy. Electrical tests and tests on a calibrated laser test stand have been performed. Both 25 and 10 μm pores MCP have been illuminated with a calibrated 408 nm laser source and measured, in terms of signal waveform, gain, and timing resolution.

III. MICRO-CHANNEL PLATE SIGNALS

Typical MCP signals measured at the two ends of a transmission line are shown in Figure 2 for a tube with 25 μm pores, for an input laser signal corresponding to 18 photo-electrons. The high voltage is set between 1.7 and 2.5 kV, depending mainly upon the pore size, and the tube is connected to the 50 Ω transmission lines on the printed circuit card. Each line reads a row of 32 anode pads at 1.6 mm pitch.
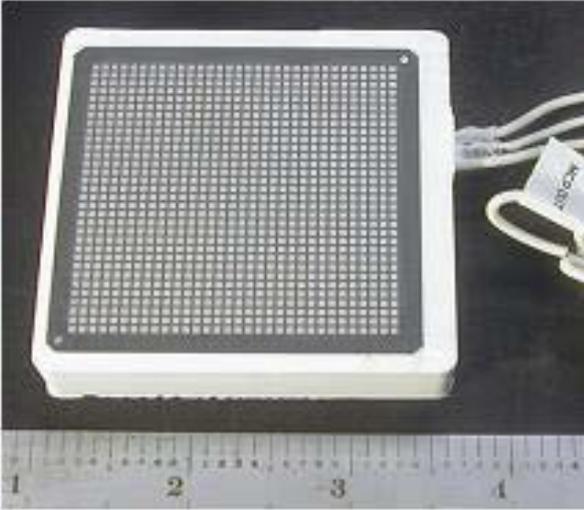
Figure 1: A 1024-anodes tube from Photonis. Bottom view showing the anodes outputs.

Figure 2: Signals from a Photonis XP85011 micro-channel plate photo detector with 25μm-diameter pores, recorded with a Tektronix TDS6154C oscilloscope using a calibrated laser test-stand. The signal corresponds to 50 photo-electrons, with a signal-to- noise ratio (average amplitude over rms noise) of 38dB. The oscilloscope analog bandwidth is 9 GHz, the sampling rate is 20 GSa/s, and the horizontal and vertical scales are 2.5 ns/division, and 5mV/division, respectively.

Each end is loaded with 50 Ω at the inputs of a fast sampling oscilloscope (Tektronix 6154C) which records the signals at 20 GSa/s sampling frequency and a 9 GHz analog bandwidth. In this particular case, the rise-time is of the order of half a nanosecond, the amplitude of the order of a few tens of millivolts. Table 1 shows the measured amplitudes and rise times for MCPs with 25 and 10 μm, at voltages of 2.0 and 2.5 kV respectively, illuminated by the laser light providing 18, 50, and 158 photo-electrons.

The laser test bench has been calibrated using a Quantacon Burle 8500 single electron resolution photo-multiplier. The laser was a PLP-10 from Hamamatsu, equipped with a 408 nm head. The light pulse duration is specified to be 70ps (FWHM).

It has been previously reported that a transmission line load allows keeping the intrinsic current pulse waveform from the micro-channel plate, compared to readout where all pads would be tied together, due to a significant reduction of the capacitances and inductances seen from each anode [1, 2].

A transmission-line readout card has been implemented on a printed circuit board (4350B from Rogers) with 32 parallel transmission lines of 50 Ω impedance at a 1.6 mm pitch, each reading one row of anode pads at the back of the tube (Figures 3, 4 and 5).

Each transmission line on the readout card is glued with conducting silver epoxy to the associated row of 32 anodes readout electronics.   Only 6 of the 32 transmission lines were brought out to SMA connectors at the edge of the card to testing purposes. The reminding lines were terminated at each end in 50 Ω.   The 32-anode pads of the MCP are stub-tied evenly over 2-inches, each pad contributing approximately a 100 fF capacitance to the line. The lossy transmission line model in the simulation was extracted from a layout of the printed circuit board by the HyperLynx simulator (Mentor-Graphics).
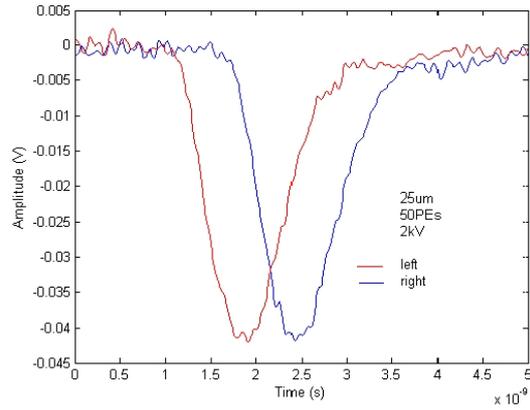
Table 1. MCP signal's amplitudes for 18, 50, and 158 photo-electrons, for 25 and 10 μm pores Micro-Channel Plates from Photonis, read with a 50 Ω transmission lines card

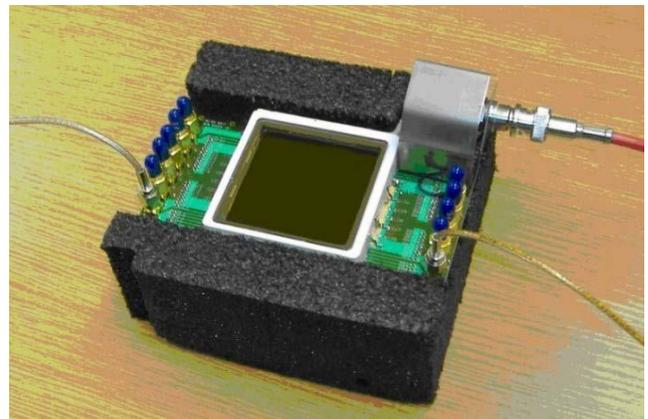| Pores and High Voltage	25μm 2kV	10μm 2.5kV
Photo-electrons	mV	mV
10	25	68
50	35	100
158	78	224

Figure 3: The transmission line card equipped with a 25 μm MCP.

Figure 6 and 7 show the simulation results. An input pulse with a 100 ps rise time is applied to the center pad. The simulation for signal integrity was setup with the equivalent representation shown in Figure 5. The input signal can be applied on any of the 32 anodes. The output voltage pulses are obtained at the 50 Ω terminations at each end. The green curve is the input pulse on the center pad; the red is the output pulse at the left end termination; the blue is the output pulse at the right end termination. The observed reflections on the input and output pulses are due to impedance discontinuities over the transmission line from the 32 stub-loaded capacitances of the MCP anodes. A 5ps/mm propagation time constant was predicted from the simulations.

Figure 7 shows a simulation of a pulse propagated through a transmission line of 1m length. From Figure 7, a propagation velocity of 5ps/mm is predicted: a 16ps time delay between left and right output was observed since the line length on the left is 1.6 mm shorter than the line length on the right side.
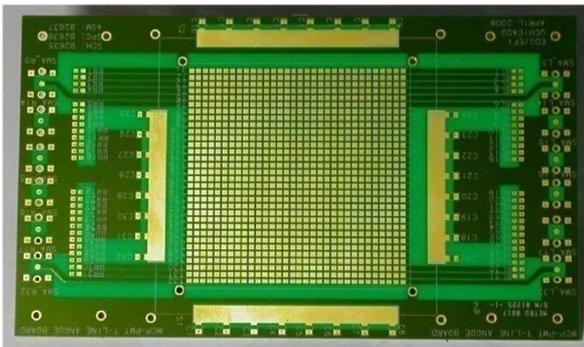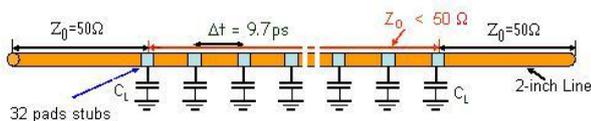

Figure 4: The 50Ω transmission lines card.

Figure 5: Electrical equivalent of the transmission line MCP readout.

The simulation shows that the transmission-line has an analog bandwidth of 3.5 GHz, well-matched to the output bandwidth of a tube with a rise-time of 100 ps.

IV. TIMING TECHNIQUES

There are a number of techniques to measure the arrival time of very fast electrical pulses [3-7, 13]. Typically one measures the time at which the pulse crosses a single threshold, or, for better resolution, the time at which the pulse reaches a constant fraction of its amplitude [7]. An extension of the threshold method is to measure the time that a pulse crosses multiple thresholds. A recent development is the large-scale implementation of fast analog waveform sampling onto arrays of storage capacitors using CMOS integrated circuits at rates on the order of a few GSa/s. Most, if not all of them, have actually 3-dB analog bandwidths below 1 GHz [8-

11]. The steady decrease in feature size and power for custom integrated circuits now opens the possibility for multi-channel chips with multi-GHz analog bandwidths, able to sample between 10 and 100 GHz, providing both time and amplitude after processing.

Assuming that the signals are recorded over a time interval from before the pulse to after the peak of the pulse with sufficient samples, the fast waveform sampling provides the information to get the time of arrival of the first photoelectrons, the shape of the leading edge, and the amplitude and integrated charge. While other techniques can give time, amplitude, or integrated charge, fast sampling has the advantage that it collects all the information, and so can support corrections for pileup, baseline shifts before the pulse, and filtering for noisy or misshapen pulses.
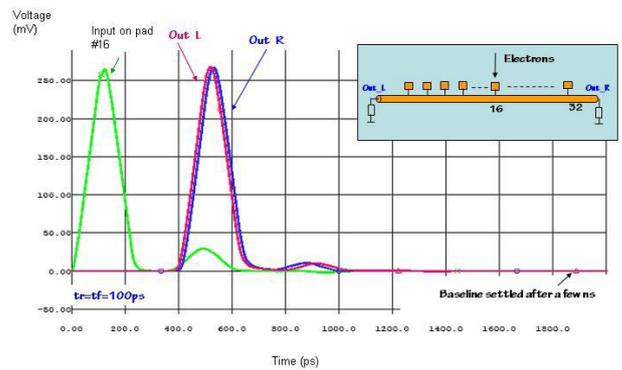

Figure 6 Simulation of the transmission line using the model of Figure 5. A 100 ps rise-time current signal is injected at the center of the transmission line (pad 16).

In addition, this method is not sensitive to base-line shifts due to 'pile-up', the overlap of a pulse with a preceding one or many, a situation common in high-rate environments such as in collider applications.
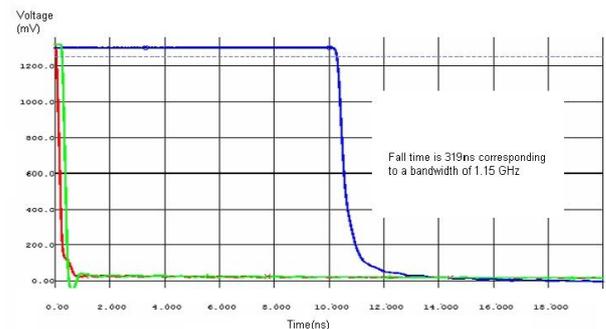

Figure 7: Simulation of the propagation of a pulse through a 1m transmission line. Red curve: the input pulse, green curve: the output on the left side, blue curve, the output on the right side.

Also, for applications in which one is searching for rare events with anomalous times, the single measured time does not give indications of possible anomalous pulse shapes due to intermittent noise, rare environmental artifacts, and other rare but real annoyances common in real experiments. In contrast, constant fraction discrimination takes into account only the pulse amplitude. The most commonly used constant fraction discriminator technique forms the difference between attenuated and delayed versions of the original signal,

followed by the detection of the zero crossing of the difference signal. There are therefore three parameters: the delay, the attenuation ratio, and the threshold. These parameters have to be carefully set with respect to the pulse characteristics in order to obtain the best timing resolution.

Waveform sampling stores successive values of the pulse waveform. For precision time-of-arrival measurements, such as considered here, one needs to fully sample at least the waveform leading edge over the peak. The sampling method is unique among the four methods in providing the pulse amplitude, the integrated charge, and figures of merit on the pulse-shape and baseline, important for detecting pile-up or spurious pulses. An iterative least-squares fit making use of a noiseless MCP template signal is then applied to the data using an algorithm that has been implemented for high resolution calorimetry measurements with Liquid Argon detectors [12,13].

V. RESULTS

Using the calibrated test bench, it has been possible to illuminate MCPs mounted on transmission lines cards as shown in Figure 4 with a controlled amount of light (408 nm), at given rates, over the whole sensitive area of the MCP photocathode.

Moving the laser light spot along a transmission line and recording the signal at the two ends of the line allows measuring both the instant (average of the two times of arrival) and the position (difference of the two times of arrival) of the impact on the photocathode. The distribution of the instants allows measuring the timing resolution of the MCP, and the distribution of the differences provides the position resolution as described below.

The spread (RMS) is on the order of 30 ps for each distribution, corresponding to the sum of different contributions: MCP transit time spread, laser jitter, oscilloscope trigger jitter, electronics system noise. Figure 8 shows 80 pulses from a 25 μm MCP recorded at 20 GSa/s at the two ends of the central transmission line. The oscilloscope was triggered by a pulse synchronous with the laser, and the two pulses were recorded on the two traces of the same trigger frame.

Figure 9 shows the histogram of the difference of the times of arrival, deduced from the sampled data using the timing extraction technique described above. The spread is on the order of a few pico-seconds, as the two signals are strongly correlated, since they originate from the same current pulse injected by the MCP's anodes at the same location in the transmission line.

The electronics system noise is the only contribution to this spread, as all others cancel out. At 158 photo-electrons, the position spread has been found to be 124μm, and the differential time spread to be 2.3ps for the 10 μm MCP at 2.5 kV. The propagation constants have been measured to be 7.6 ps/mm for the 25 μm MCP, and 9.3 ps/mm for the 10 μm MCP, at 2.0 and 2.5 kV respectively.

Figure 10 shows the measured position resolution versus the high voltage for the 25 μm MCP and a light input corresponding to 158 photo-electrons. Figure 11 shows the position spread versus the position of the light spot along the

transmission lines, for both MCPs, at 18 and 50 photo-electrons.
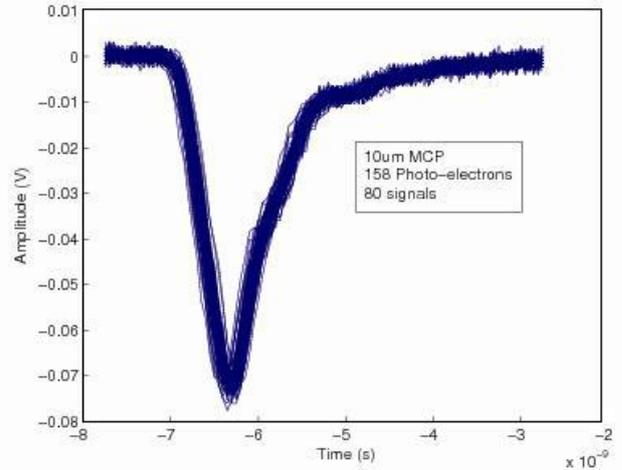

Figure 8: Traces from 80 measured pulses at one end of the central transmission line. The large spread in time of arrival is mainly due to the laser jitter triggering the oscilloscope.

VI. SUMMARY AND CONCLUSIONS

We have shown that Micro-Channel Plate detectors coupled to fast transmission lines read with waveform sampling can measure the position along the lines with accuracy well below 1 mm.

The measurements agree well with simulations based on templates derived from real signal shapes and theoretical modeling of the transmission line electrical characteristics. The readout scheme of transmission lines with impedance matched waveform sampling at each end allows using MCP-based photo-detectors for large area sensors in which several devices could be read in series, reducing significantly the number of electronics channels, and consequently the power, the on-detector material, and the amount of data.
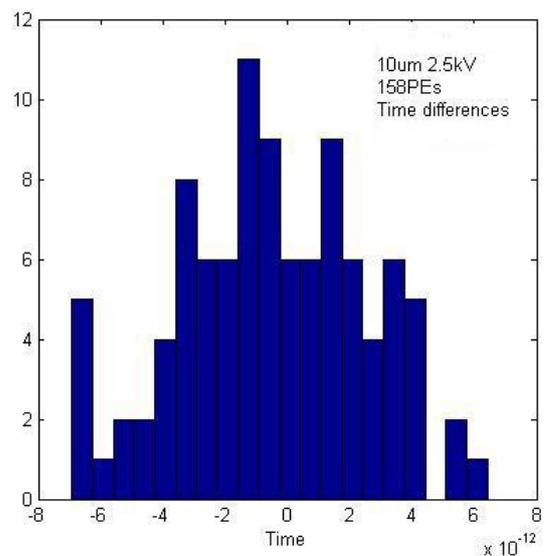

Figure 9: The histogram of the measured times of arrival differences deduced from the sampled data processed with the algorithm from [12]. RMS is 2.3ps corresponding to a position spread of 125μm
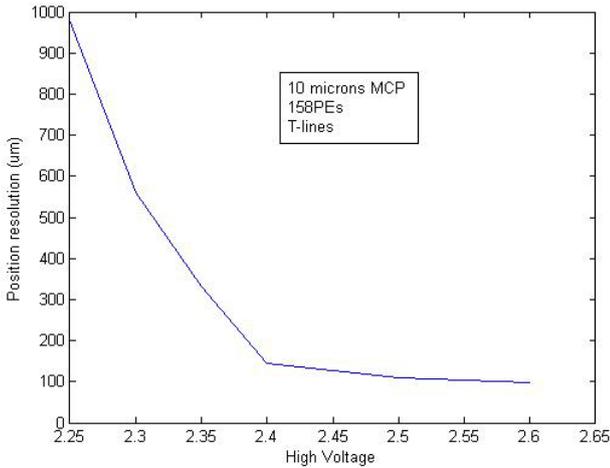
Figure 10: The histogram of the measured times of arrival differences deduced from the sampled data processed with the algorithm from [12]. RMS is 2.3ps corresponding to a position spread of 125μm.
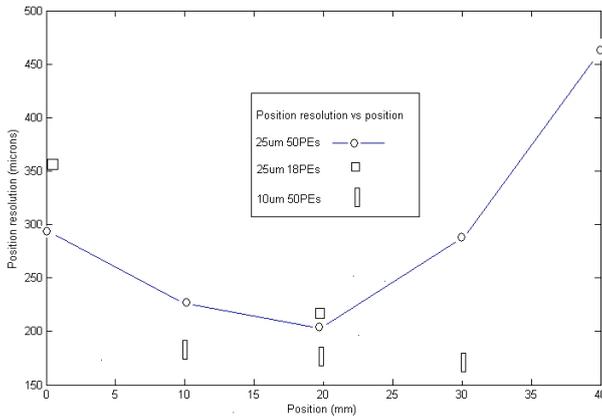

Figure 11: Measured position resolution versus position at 18 and 50 Photo-electrons between 5 and 45 mm from the side of the MCP.

ACKNOWLEDGEMENTS

VII.   REFERENCES

[1]   C. Ertley, J. Anderson, K. Byrum, G. Drake, E. May, http://www.hep.anl.gov/ertley/windex.html
[2]   F. Tang, J. Anderson, K. Byrum, G. Drake, C. Ertley, H.J. Frisch, J-F. Genat, "Transmission line readout with Good Time and Space resolutions for Planacon MCP-PMT"; *Proceedings of the TWEPP-08 Workshop*, Naxos, Greece, 2008, pp. 579-581
[3]   D.I. Porat, "Review Of Sub-nanosecond Time Interval Measurements"; *IEEE Trans. Nucl. Sci.* 1973, pp. 36-.
[4]   J-F. Genat, " High Resolution Time to Digital Converters"; *Nucl. Inst. Meth*. A315, 1992, pp. 411-414.
[5]   J. Kalisz, "Review of Methods for Time Interval Measurements with Picosecond Resolution"; Institute of Physics Publishing, *Metrologia,* 41, 2004, pp. 17-32.
[6]   An extensive list of references on timing measurements can be found in: A. Mantyniemi, MS Thesis, Univ. of Oulu, 2004; ISBN 951-42-7460-I; ISBN 951-42-7460-X; http://herkules.oulu.fi/isbn951427461X/isbn951427461X.pdf
[7]   S. Cova et al., "Constant Fraction Circuits for Picosecond Photon Timing with Micro-channel Plate Photomultipliers"; *Review of Scientific Instruments*, 64-1, 1993, pp. 118-124.
[8]   D. Breton, E. Auge, E. Delagnes, J. Parsons, W. Sippach, V. Tocut, "The HAMAC rad-hard Switched Capacitor Array"; ATLAS note, CERN 2001.
[9]   E. Delagnes, Y. Degerli, P. Goret, P. Nayman, F. Toussenel, and P. Vincent, "SAM : A new GHz sampling ASIC for the HESS-II Front-End"; Cerenkov Workshop, 2005.
[10]   S. Ritt, " Design and Performance of the 5 GHz Waveform Digitizer Chip DRS3"; Submitted to *Nuclear Instruments and Methods*, 2007.
[11]   G. Varner, L.L. Rudman, A. Wong, "The First version Buffered Large Analog Bandwidth (BLAB1) ASIC for high Luminosity Colliders and Extensive Radio Neutrino Detectors" ; Nucl. *Inst. Meth*. A591, 2008 pp. 534.
[12]   W.E. Cleland and E.G. Stern, "Signal Processing considerations for Liquid Ionization Calorimeters in a High Rate Environment"; *Nucl. Instr. Meth*. A338, 1994, pp. 467-497.
[13]   J-F. Genat, G. Varner, F. Tang, H.J. Frisch, "Signal Processing for Picosecond Resolution Timing Measurements"; Submitted to *Nuclear. Instruments and Methods*.